RESEARCH ARTICLE

Chitosan–hydroxyapatite macroporous matrix for bone tissue engineering

Sun Mi Zo[1,2], Deepti Singh[1,2], Ashok Kumar[3], Yong Woo Cho[4], Tae Hwan Oh[1,2] and Sung Soo Han[1,2,*]

[1]Department of Nano, Medical and Polymer Materials, College of Engineering, Yeungnam University, 214-1 Daedong, Gyeongsan 712749, Korea
[2]Polymer Gel Research Cluster Center, Yeungnam University, Gyeongsan 712749, Korea
[3]Indian Institute of Technology Kanpur, Kanpur 208 016, India
[4]Department of Chemical Engineering, Hanyang University, Ansan, Gyeonggi-do 426791, Korea

In recent years, bone tissue engineering which involves cells, three-dimensional (3-D) matrix and/or recombinant signalling molecules has been extensively studied to find an ideal bone implant. The scaffold for bone tissue engineering should be porous to allow mass transfer at high rate along with mechanical property in par with bone structure to ensure integrity of neo-tissue. In this work, we have combined well-known hydroxyapatite ($Ca_{10}(PO_4)_6(OH)_2$; HA) and chitosan that provides ideal surface chemistry for its osteoblast attachment and enhances mineralization and is known for its osteoconductive and osteoinductive properties. We have synthesized chitosan–hydroxyapatite (CH–HA) macroporous scaffold, in simple two-step process, using freeze-drying technique. Scanning electron microscope analysis showed macroporous architecture with interconnected pores. EMAX testing for elemental analysis clearly indicated presence of calcium, phosphorus and sodium along with oxygen and nitrogen in the scaffold. The Fourier's transmission infrared spectroscopy (FTIR) examination showed chemical bonding between both the polymers. To further evaluate 3-D profiling of CH–HA scaffold, rheological testing was performed which showed no significant change in G', G'' and phase angle proving mechanical stability of the material which was able to bear stress without leading to deformation. Human osteoblast seeded on CH–HA matrices showed enhanced cellular proliferation and viability for longer period of time. Increased mineral deposition was examined using alkaline phosphatase assay which confirmed that CH–HA scaffold provided conducive environment for osteoblast proliferation and mineral deposition. The mechanical properties and microarchitecture of the scaffold were found to be ideal for bone tissue engineering.

Keywords: Bone tissue engineering, chitosan–hydroxyapatite, EMAX elemental analysis, macroporous, rheology.

TISSUE engineering principally applies the material engineering and biological sciences concept to create artificial constructs that regenerate neo-tissues[1,2]. A three-dimensional (3-D) scaffold plays an impetus role in scaffold-assisted tissue regeneration[3,4]. The scaffolds until recently were perceived as only cell carriers however, in contrast, these materials have shown to govern the fate of cells and ultimately decide the outcome of the process. Along with acting as artificial extracellular matrix for cellular attachment and proliferation, scaffold microarchitecture and surface property have influenced cell behaviour, differentiation and neo-tissue formation[5–7]. There are numerous fabrication techniques for scaffolding and in the recent past, efforts have been made to improve the surface of the scaffold both in terms of its topography and chemistry that can make a scaffold ideal for desired applications and has a pronounced effect both in *in vitro* and *in vivo* systems[8]. Designing an ideal scaffold in tissue engineering is challenging as every step from polymer choice to fabrication and characterization influences the regeneration of the tissue[9,10]. In case of load-bearing tissues of the body, bone regeneration and repair is most common, yet complicated process. In spite of various allograft and autograft techniques along with prosthesis, it has its own limitation spanning from donor storage to immune reaction to null bone regeneration[11–14].

Bone tissue engineering is an ideal substitute for treating bone defects and has been heralded as an alternative to bone regeneration[15] as it combines bone cells (osteoblast or pre-osteoblast) and a biodegradable 3-D scaffold to repair damaged or disease bones. Success of this approach mainly depends upon the size of the defect that needs repair along with fabrication of 3-D fully integrated, internal channels with controlled interconnected porous structure that can match the stiffness of the surrounding bone to avoid stress shielding[16]. Unlike other 3-D scaffolds, the basic polymers of choice in bone tissue engineering are bioactive composites which exhibit osteoinductive and osteoconductive properties. In nature, the bone is a complex of organic–inorganic materials such as collagen fibrils, nano-crystallites and hydroxyapatite (HA, $Ca_{10}(PO_4)_6(OH)_2$) in a hierarchical architecture

*For correspondence. (e-mail: sshan@yu.ac.kr)

layered over several length scales[17–20]. There are different classes of bioactives depending upon the bioactivity index and HA belongs to class A due to its ability to bind to both hard and soft connective tissues[21]. Class A materials possess both osteoconductive and osteogenetic properties, whereas class B materials exhibit only osteoconductive behaviuor[22]. HA consists of basic components such as phosphorus (P) and calcium (Ca) that induce intra- and extracellular responses[23]. HA along with some natural polymer combination is found to be one of the ideal scaffolds for tissue engineering. Among the major natural polymers used, chitosan (CH) has been exhaustively used in all scaffolds intended for major load-bearing tissues of the body[24]. These next-generation materials combine the ideal bioactive and natural polymer composited which mimics natural bone functions and activates *in vivo* tissue regeneration mechanism[25]. CH is a natural polysaccharide derived mostly from crab shell, but can also be obtained from shrimps, coral and jellyfish. CH is an ideal polymer for biomedical application due to its biocompatible and bio-degradation properties along with osteoconduction and intrinsic antibacterial nature. CH has been applied in cartilage tissue engineering[26,27], wound healing[28] and bone or orthopaedic applications[29,30].

In this study, we report fabrication of chitosan–hydroxyapatite (CH–HA) macroporous interconnected structure along with the distribution of polymers, chemical bonding, rheological properties of the material, cell proliferation and alkaline phosphatase activity of the macroporous scaffold designed in simple two-step process. The freeze-drying technique for scaffold fabrication has resulted in macroporous, interconnected network of polymer matrix that supports human osteoblast attachment and proliferation and early onset of bone mineralization and subsequent extracellular matrix deposition.

Material and methods

CH, HA, Dulbecco's modified Eagle's medium (DMEM), 3-(4,5-dimethylthiazol-2-yl)-2,5-diphenyltetrazolium bromide (MTT), glutaraldehyde (50%), trypsin–EDTA, foetal bovine serum, penicillin–streptomycin, nystatin and DAPI were purchased from Sigma Aldrich (St Louis, Mo, USA), NaOH from Duksan Pvt Ltd (South Korea). Human osteoblast cells (hFOB) were purchased from ATCC (Manassas, VA, USA). Alkaline phosphatase Kit (AbCAM, USA) and Live/Dead viability/cytotoxicity Kit were purchased from Life Technology, Invitrogen, USA. All the other chemicals used were of analytical grade.

Optimizing polymer concentration for scaffold fabrication

CH (200 mg) was weighed and dissolved in 10 ml of 1% acetic acid solution at high temperature (~ 80°C) to completely dissolve the polymer. Under continuous stirring, 1% HA was added to the polymer solution and incubated at –20°C for 24 h. Following incubation, the scaffold was dipped into 10% NaOH solution for 8 h. Scaffolds are washed with double distilled (DD) H_2O until neutralized and dried until further used.

Microstructure and elemental analysis

Morphology of the scaffold was studied using scanning electron microscopy (SEM, Hitachi S-4100). CH–HA scaffold was coated with platinum using ion sputter coater (Hitachi E-1030). SEM was operated under high vacuum at 15 kV with sample spot size of 5 mm to image the samples. EMAX (Horiba) SEM-associated software (microanalysis suite) was further used for elemental analysis of scanned samples choosing random regions of CH–HA scaffold. Along with average pore size, interconnectivity and pore-diameter, distribution of CH and HA in a 3-D system was determined by this procedure.

Chemical interaction by FTIR

FTIR (PerkinElmer Spectrum 100 – USA) was used for obtaining infrared spectrum of the CH–HA scaffold. Briefly, 2 mm section of the scaffold was used for the analysis and peaks were further plotted after obtaining the spectra.

Rheology of CH–HA scaffold

Rheology analysis is used to measure visco-elastic property of the material and deformation under given conditions[5]. Device (Rheometric scientific serial no: 4X841702PCE) was used for characterization of CH–HA scaffold. All polymeric materials display characteristic behaviour under stress and different temperatures. CH–HA scaffold sections were cut and placed on sample holder with gap width of 150 μm and force applied was 1 N per second at constant temperature. Graph was plotted with loss modulus (G'), storage modulus (G'') and phase angle.

Human osteoblast responses to CH–HA matrix

CH–HA scaffold was treated with gradient ethanol for sterilization. CH–HA 5 mm sections were cut and pre-equilibrated with phosphate buffer saline (PBS) (0.1 M, pH 7.4) followed by DMEM cell-culture media. Human osteoblast cells (hFOB) were seeded on to CH–HA with cell seeding density of 1×10^4 cells/well/scaffold. Experiment was set up in triplicate with two-dimensional (2-D) cell culture treated 24-well plate as control. 3-(4,5-dimethylthiazol-2-yl)-2,5-diphenyltetrazolium bromide

(MTT) assay was performed on every 5th day of the experiment to check for metabolic activity of the cells. MTT is an indirect assay for checking cell growth, proliferation and metabolic activity of cells. The mitochondrial enzyme of metabolically active cells oxidizes MTT resulting in development of a purple or dark violet colour product. Briefly, MTT was dissolved in DMEM (without foetal bovine serum (FBS)) and added to the scaffold and 2-D system and incubated for 4 h. After incubation, MTT was gently aspirated out and dimethyl sulphoxide (DMSO) (1 : 3) added to each test to dissolve intraformazan crystals and obtain the end product, which can be read spectrophotometrically at 490 nm.

Cell–matrix interaction

Scaffold seeded with hFOB was fixed with 2.5% glutaraldehyde after completely removing the media. Live–dead staining kit was used to evaluate the cell–matrix interaction. Ethidium bromide (2 mM) was diluted in 10 ml distilled tissue culture grade PBS in combination with 4 μm of calcein acetomethoxy (calcein AM) from stock solution. The working solution of the stain 100–150 μl was added and incubated for 30 min and labelled cells were observed under Nikon fluorescent microscope.

Functionality assay: alkaline phosphatase activity

Alkaline phosphatase (ALP) activity was evaluated by a functionality assay using ρ-nitrophenyl phosphatase as substrate (AbCAM protocol). Absorbance was read spectrophotometrically at 405 nm. ALP was directly converted from the absorbance plotted using standard curve (serum albumin) with concentration varying from 0.1 to 1.0 mg/mol.

Statistical analysis

Statistical analysis of all the chemical and biological experiments on the scaffold was performed in triplicates. All the experimental values were expressed in the form of mean ± standard deviation. The results were statistically compared using SPSS 20 for independent *t*-tests and the values of $p < 0.05$ were considered as statistically significant.

Results and discussion

Scaffold fabrication and mechanical strength

A number of composites have been synthesized using CH and HA[31,32] using co-precipitation[13] or sintering methods[33]. However, this is the first time we report a macroporous scaffold with interconnected pores, ideal mechanical strength with high osteoblastic activity synthesized in a two-step process using freeze-drying technique. Series of scaffolds were fabricated by using freeze-drying technique (Figure 1) with different concentrations of CH and HA to obtain a scaffold with ideal physico-chemical properties to suit the desired application. Porous 3-D scaffold is considered to be most suitable for tissue engineering, considering this the final concentration of polymers was found to be 2 : 1. SEM image revealed interconnected porous network of polymers (Figure 2) with pore size ranging from 50 to 110 μm; average pore size being 85 μm, which is most suitable for bone tissue engineering. CH–HA scaffold has been synthesized as a membrane using co-precipitation process and the pore size of this composite was found to be approximately 50 μm (ref. 13). The freeze-drying process for CH–HA scaffold fabrication is simple, easier and controlled porous structure could be obtained by manipulating the polymer concentration and freezing temperature.

Elemental analysis of the scaffold by EMAX

SEM-associated EMAX software was used to check for elemental distribution. Five scaffold sections of 2 mm were dried, platinum-coated and random regions were scanned for examining the distribution and interaction of CH and HA. EMAX software revealed peaks of sodium (Na), phosphorus (P), calcium (Ca), oxygen (O) and nitrogen (N) along the length of the scaffold. These elements were present in all random regions of the five samples (Figure 3). HA is a natural mineral component composed of calcium apatite with phosphorus and calcium as monomers. Distribution of CH–HA indicates homogenous mixing and interaction of both polymers was achieved using freeze-drying technique.

Chemical interaction of CH–HA: FTIR

FTIR was performed to identify important interactions between natural polymer CH and bioactive component HA. FTIR examination reveals peaks at 1463 and 1558 cm^{-1} revealing C=O stretching and strong peak at 2848 and 2916 cm^{-1} which belongs to C–H stretching region and small peaks between 2160 and 2255 cm^{-1} corresponding to C=C along with peaks at 1084 and 2848 cm^{-1} indicating amide II band. Peaks at 1073 and 1117 cm^{-1} are typically PO_4 corresponding to different vibration modes of phosphate group in HA (Figure 4). HA also contains carbonate ions which can be clearly observed during FTIR analysis. Peaks seen at 1654, 1598 and 1550 cm^{-1} are assigned to amide I (C=O), amino ($–NH_2$) and amide II (–NH) respectively. FTIR results clearly indicate the strong bonding between the CH and HA moiety, achieved by a simple two-step scaffold fabrication process.

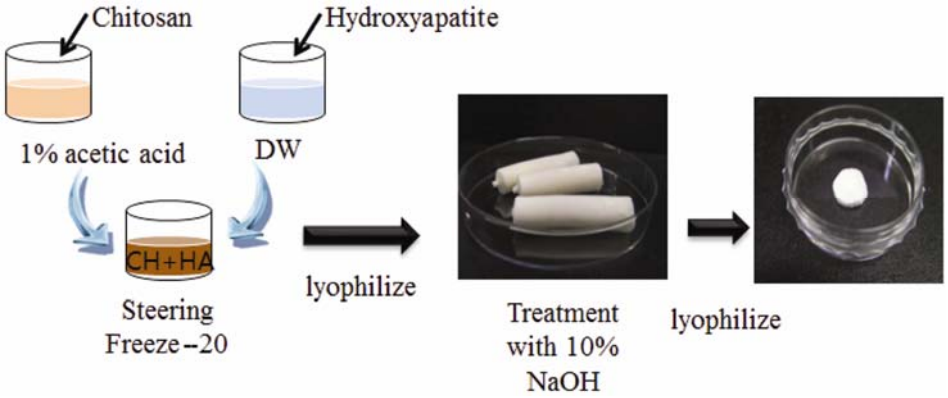

Figure 1. Schematic representation of steps involved in fabrication of CH–HA macroporous scaffold.

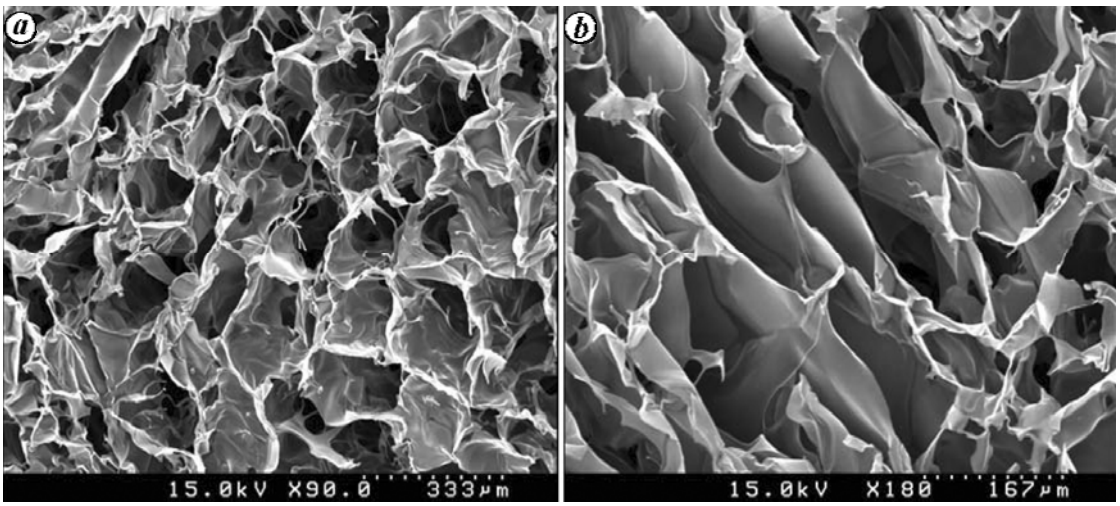

Figure 2. Scanning electron micrograph image showing porous and interconnected network of CH–HA scaffold.

Rheology of CH–HA scaffold

Rheology is simply defined as study of the deformation and flow of material. It has been used to understand the complex structure of various materials such as polymers, suspension and body-fluid. Briefly, rheology can be defined as a relationship between deformation/flow, internal structure and performance of the material which cannot be defined in terms of a single value of classic fluid mechanics. When a material is subjected to different stresses, each material responds in various ways expressed as either elasticity or viscosity of the material; however, between these two, lies a third property whose dual nature is known as visco-elastic behaviour of the material. The solid behaviour of the material is termed as storage modulus (G'), liquid behaviour is depicted as loss modulus (G''), which is derived with the equation given below[5].

$$G' = \left.\frac{\text{In-phase stress}}{\text{Maximum strain}}\right\} \text{Storage modulus,}$$

$$G'' = \left.\frac{\text{Out of phase stress}}{\text{Maximum strain}}\right\} \text{Loss modulus.}$$

Rheology study of CH–HA scaffold confirmed the stable nature of the material when subjected to different stresses and temperatures. CH–HA scaffolds were able to bear increased stress without deforming and with increasing temperature, no significant change in the values of G' and G'' was observed. G' value was found to be stable around 10^3 (Figure 5). This study shows the ability of the scaffold to bear stress without deforming, showing the mechanical stability and stiffness of the material which could be ideal for bone and cartilage tissues.

Solvent adsorption and swelling kinetics

Interconnected porous network is needed for nutrient and mass transport during cell culture set-up[34] and to understand the complex architecture of the scaffold pores solvent adsorption study was performed on four samples.

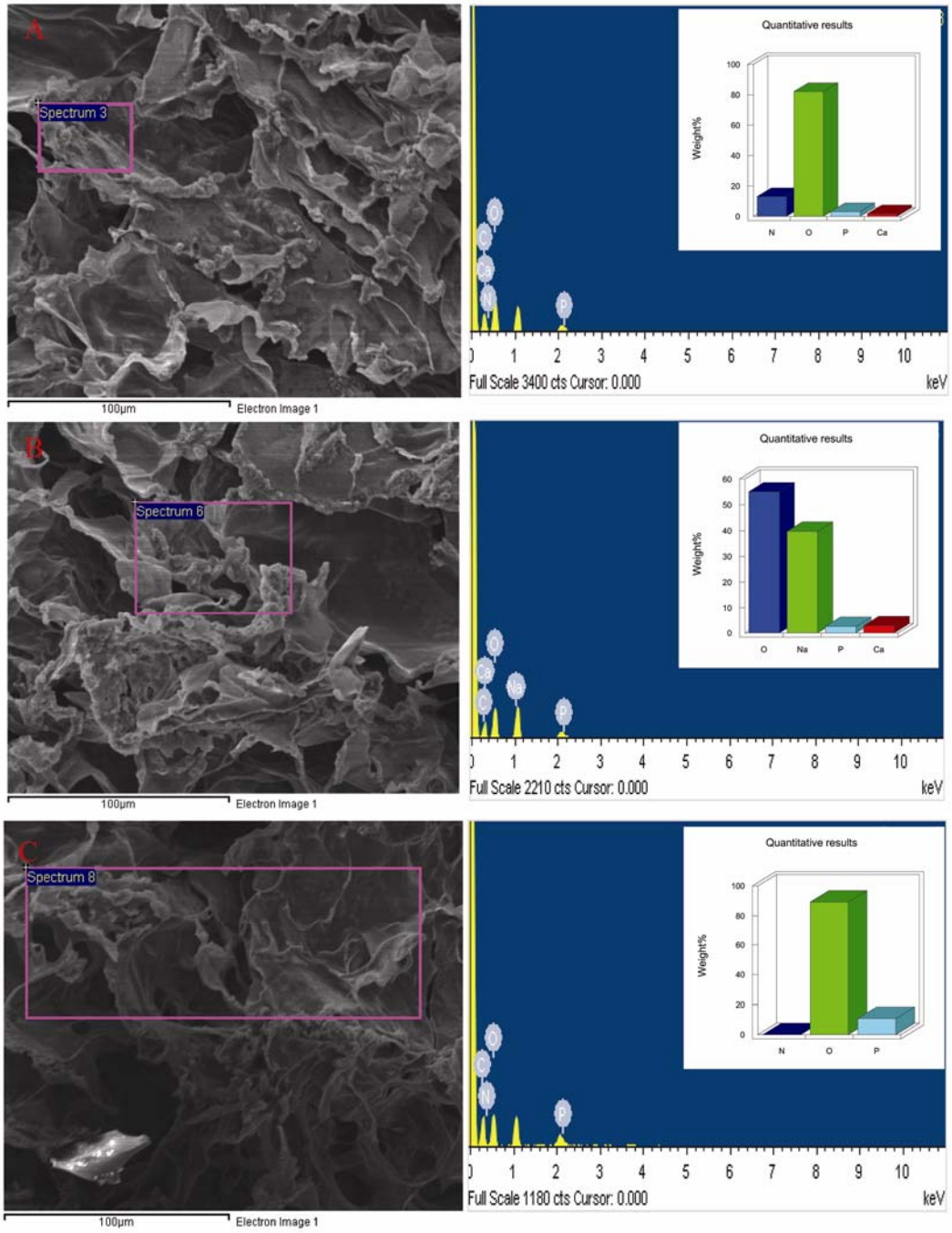

Figure 3. Elemental analysis using EMAX software of different areas of CH–HA scaffold shows presence of sodium (Na), phosphorus (P), calcium (Ca) with oxygen (O) and nitrogen (N).

Lyophilized dried gels used for swelling kinetics were saturated with DD H_2O at room temperature. CH–HA scaffold swelled up to 80% from its original weight within 90 sec and attained equilibrium at 120 sec with swelling of 94% (Figure 6). Four samples were used for the experiment to obtain concurrent reading with average swelling ratio of 8.5 ± 0.32. High water uptake capacity and swelling ratio of CH–HA suggested a large-pores scaffold with interconnected porous architecture.

Human osteoblast response to CH–HA matrix

In vitro cellular response to the matrix was evaluated by seeding human osteoblast cells. CH–HA scaffolds were pre-equilibrated with cell-culture media and 1×10^4 cells/well/scaffolds was seeded on to a 5 mm section. The experiment was set up for 30 days with 2-D as control and metabolic activities were monitored using MTT assay and functional activity using ALP levels. ALP is a known

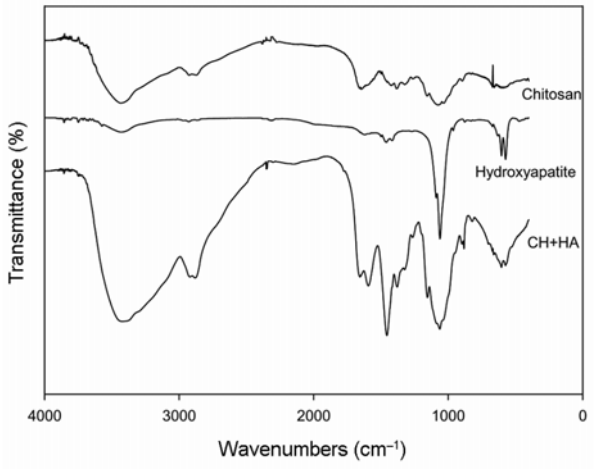

Figure 4. Fourier's transmission infrared spectroscopy examination reveals corresponding peaks to different vibration modes of phosphate group in HA and CH.

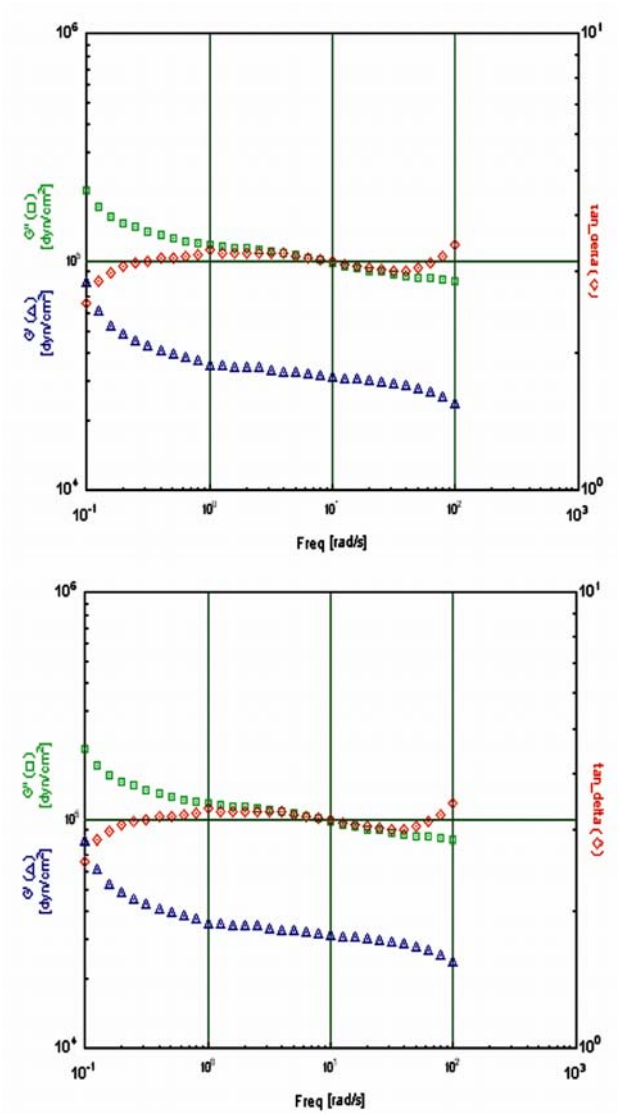

Figure 5. Rheology performed to check the visco-elastic property of the CH–HA scaffold showed no significant change in loss modulus (G''), storage modulus (G') and phase angle.

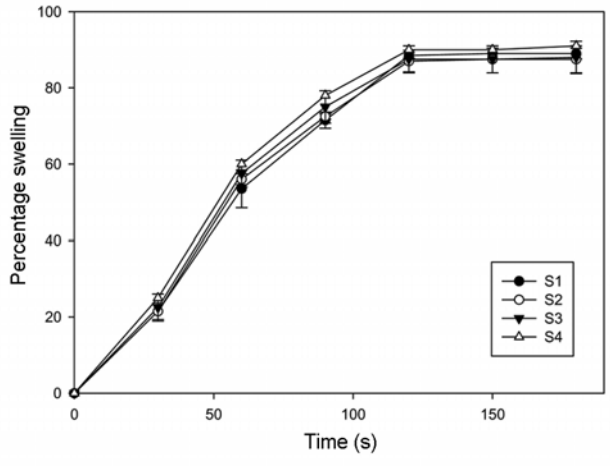

Figure 6. Swelling kinetics of the CH scaffold was performed on four samples repeatedly dried and swelled in PBS. The swelling kinetics showed high water uptake capacity and scaffolds swelled up to 93% from the original weight within 120 sec. The experiment was performed in quadruplets and 'p' value was < 0.05.

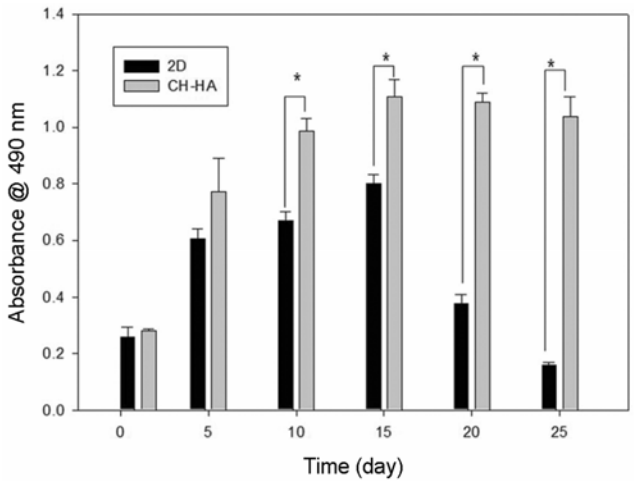

Figure 7. MTT assay performed on regular time interval shows steady increase in metabolic activity of osteoblast seeded on CH–HA scaffold compared to 2-D system.

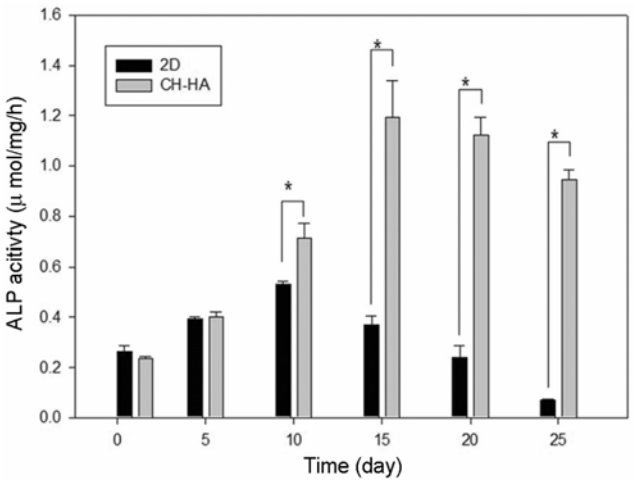

Figure 8. The functional assay was performed by checking ALP level at regular intervals for 25 days. The osteoblast seeded on CH–HA scaffold shows elevated levels of ALP activity for 10th day onwards.

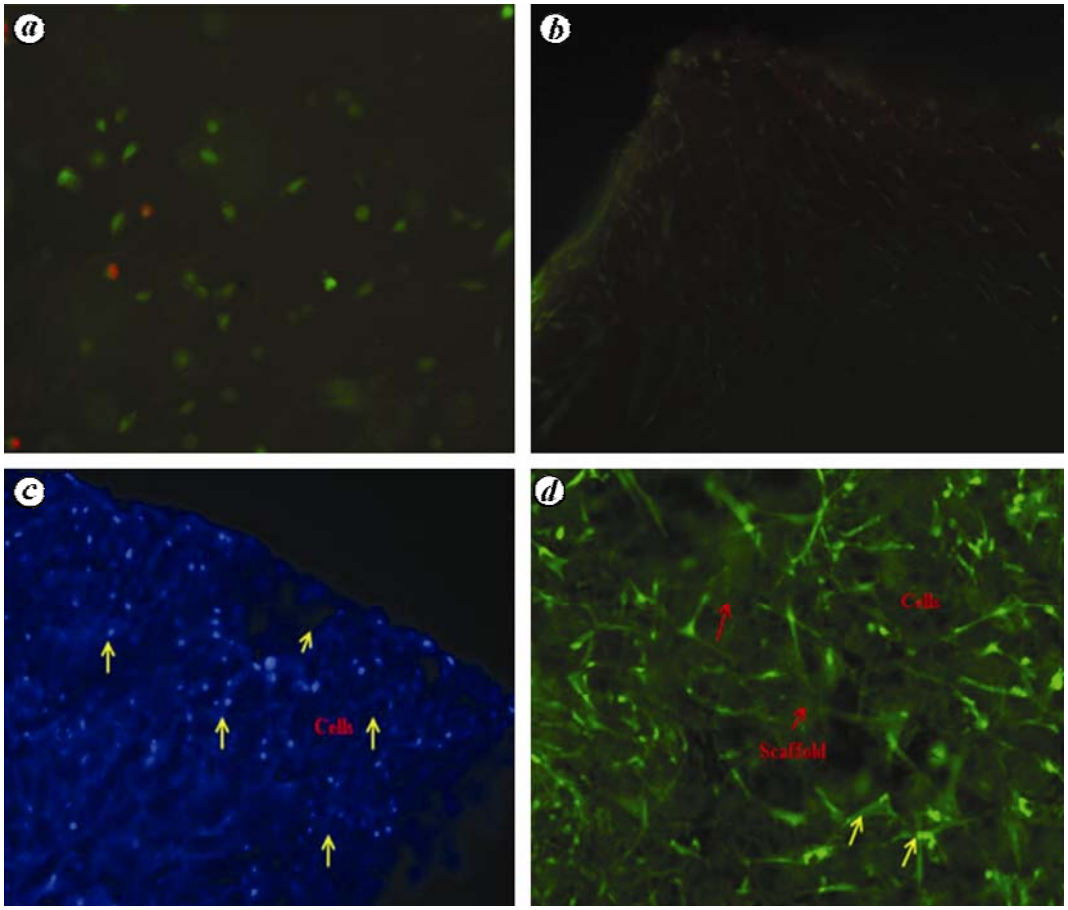

Figure 9. Fluorescent image of osteoblast interaction with CH–HA scaffold. ***a***, ***b***, Live/dead staining performed on 1st and 10th days respectively. ***c***, DAPI nuclei staining shows cell attachment on CH–HA scaffold on 15th day. ***d***, Phalloidin staining was performed for cytoskeletal stain showing high osteoblast proliferation on CH–HA scaffold on 25th day.

marker used for differentiation of osteoblast cells at a relatively early bone formation stage[35] during mineralization and matrix protein formation and has been a widely accepted marker for evaluating the performance of biomaterials, especially designed for bone tissue engineering. MTT assay performed on every 5th day of the experiment shows slow increase in metabolic activity of osteoblasts which is mainly attributed to the fact that osteoblasts are slow proliferating cells by nature. Steady increase in the absorbance was found to be indirectly related to the higher rate of cell proliferation; however in the 2-D system, osteoblast showed increasing trend during first half of the experiment set-up and later the rate was seen to decline (Figure 7).

Functionality assay: ALP and live/dead analysis

ALP activity showed upward trend from 10th to 20th days of the culture (Figure 8). CH–HA with mechanical stability and compression modulus similar to bone tissue were found to be ideal for cell attachment and proliferation and ALP levels suggested that matrix was more favourable for differentiation of osteoblast during culture resulting in increased level of ALP in the cells of the scaffold, in comparison to the 2-D system. Live cells possess ubiquitous intercellular esterase activity, which is determined by the ability to convert cell permeate non-fluorescent calcein AM into intensely fluorescent calcein. Polyanionic calcein dye is retained within live cells, producing intense green fluorescence at ~495/515 nm, whereas ethidium bromide can penetrate only dead or damaged cells and undergoes ~40-fold increment in fluorescent intensity upon binding to nucleic acid which results in red fluorescence in dead cells. Cell viability/cytotoxicity examined on 1st and 10th days using live/dead staining kit, showed high number of cell viable green cells (Figure 9 *a* and *b*). DAPI and cell tracker used to stain the nuclei and cytoskeleton of cells respectively, showed higher number of proliferating cells on 15th and 25th days of culture (Figure 9 *c* and *d*), the cells were polygonal and did not exhibit the flattened morphology generally seen in dedifferentiated osteoblasts. Metabolic and functional activity expressed by osteoblast seeded on CH–HA scaffold indicated that these cell–matrix interactions have strong-bone forming ability in less time,

thereby shortening the healing time and improving the effectiveness of the approach towards bone tissue regeneration therapy.

Discussion

CH and HA composites have been synthesized using co-precipitation by Yamaguchi *et al.*[36], by one-step dropping of CH solution into calcium hydroxide suspension; however, these scaffolds were not macroporous, which is a requisite for tissue engineering. Few other research groups have fabricated CH–HA scaffold in the form of membranes, multilayered or microspheres[37]; however, these scaffolds need further modifications to be applied for bone tissue. We have synthesized macroporous scaffold using freeze-drying technique to obtain macroporous interconnected network in a simple two-step process. Using freeze-drying technique for fabrication of CH–HA, no further modification was needed for the scaffold as the high affinity of CH for HA with hydrophilic entity facilitates homogenous distribution of HA in aqueous solution along with facilitating the cell attachment and proliferation[38] and *in vitro* biocompatibility showed potential use of the scaffold in bone regeneration. Surface energy and hydroxyl group of HA further promotes cell attachment and proliferation, which in turn increases the DNA content of the cells during long-term culture and enhanced osteogenic differentiation; however, in case of nanoparticle or coating, the HA tends to leach, out of the scaffold, thereby reducing the effect during long-term culture. This study underscores the effect of cross-linking CH and HA and could be a potential approach to increase the mechanical strength and improve functionality of the osteoblast, thereby enhancing the mineralization process by providing the microenvironment and simultaneously preventing the dedifferentiation of cells. The challenges of tissue engineering are primarily the physicochemical properties of the scaffold, surface chemistry and biological adaptation for cell culture along with *in vivo* implantation. In line with these 3-D cross-linked CH–HA scaffold are promising substrate for bone regeneration with relatively easier for fabrication making it an ideal tissue engineering matrix.

Conclusion

In this study, we have fabricated CH–HA scaffolds of different concentrations and optimized a ratio that resulted in a mechanically stable matrix. Cross-linking using NaOH which is non-toxic and easily neutralized from the matrix results in ideal scaffold fabrication by freeze-drying technique in a simple two-step process. FTIR revealed the bonding between CH and HA and EMAX demonstrated uniform distribution of both the polymers in 3-D system. SEM examination along with swelling kinetics clearly shows that macroporous interconnected network of polymers could be achieved in two steps. The mechanical, biological and physico-chemical properties are the most important paradigm of biomaterials in tissue engineering as these matrices need to support unhindered nutrient transport, gaseous exchange with convective flow. The metabolic and functional activities tested by seeding osteoblast showed high metabolically active cells, followed by high functional activity of cells on these matrices, confirming potentiality of the CH–HA scaffold in the field of bone tissue engineering.

1. Williams, D., Benefit and risk in tissue engineering. *Mater. Today*, 2004, **7**, 24–29.
2. Rezwan, K., Chen, Q. Z., Blaker, J. J. and Boccaccini, A. R., Biodegradable and bioactive porous polymer/inorganic composite scaffolds for bone tissue engineering. *Biomaterials*, 2006, **27**, 3413–3431.
3. Mano, J. F., Sousa, R. A., Boesel, L. F., Neves, N. M. and Reis, R. L., Bioinert, biodegradable and injectable polymeric matrix composites for hard tissue replacement: state of the art and recent developments. *Compos. Sci. Technol*., 2004, **64**, 789–817.
4. Shin, H., Jo, S. and Mikos, A. G., Biomimetic materials for tissue engineering. *Biomaterials*, 2003, **24**, 4353–4364.
5. Deepti, S., Vijayashree, N. and Ashok, K., Proliferation of myoblast skeletal cells on three-dimensional supermacroporous cryogels. *Int. J. Biol. Sci*., 2010, **6**, 371–381.
6. Deepti, S., Anuj, T., Vijayashree, N. and Ashok, K., Proliferation of chondrocytes on a 3-D modelled macroporous poly(hydroxyethyl methacrylate)-gelatin cryogel. *J. Biomater. Sci. Polym. Edn*., 2011, **22**, 1733–1751.
7. Takuya, M., Ami, M., Miki, K., Shin-suke, Y., Jun-ichi, S. and Takayoshi, N., Cell-based fabrication of organic/inorganic composite gel material. *Materials*, 2011, **4**, 327–338.
8. Wang, D. A. *et al.*, Multifunctional chondroitin sulphate for cartilage tissue-biomaterial integration. *Nat. Mater*., 2007, **6**, 385–392.
9. Kanczler, J. M. *et al.*, Biocompatibility and osteogenic potential of human fetal femur-derived cells on surface selective laser sintered scaffolds. *Acta Biomater*., 2009, **5**, 2063–2071.
10. Kawai, T. *et al.*, Synthetic octacalcium phosphate augments bone regeneration correlated with its content in collagen scaffold. *Tissue Eng. Part A*, 2009, **15**, 23–32.
11. Yoneda, M., Terai, H., Imai, Y., Okada, T., Nozaki, K., Inoue, H., Miyamoto, S. and Takaoka, K., Repair of an intercalated long bone defect with a synthetic biodegradable bone-inducing implant. *Biomaterials*, 2005, **26**, 5145–5152.
12. Hae-won, K., Byung-ho, Y. and Hyoun-ee, K., Microsphere of apatite–gelatin nanocomposite as bone regenerative filler. *J. Mater. Sci. Mater. Med*., 2005, **16**, 1105–1109.
13. Shu-hua, T., Eun-jung, L., Byung-ho, Y., Du-sik, S., Houn-ea, K. and Joong-soo, O., Chitosan/nanohydroxyapatite composite membranes via dynamic filtration for guided bone regeneration. *J. Biomed. Mater. Res*., 2008, **88**, 569–580.
14. Sandberg, E., Dahlin, C. and Linde, A., Bone regeneration by the osteopromotion technique using bioabsorbable membranes: an experimental study in rats. *J. Oral. Maxillofac. Surg*., 1993, **51**, 1106–1114.
15. Rose, F. R. A. J. and Oreffo, R. O. C., Bone tissue engineering: hope vs hype. *Biochem. Biophys. Res. Commun*., 2002, **292**, 1–7.
16. Chen, Q. Z., Thompson, I. D. and Boccaccini, A. R., 45S5 Bioglass (R)-derived glass-ceramic scaffolds for bone tissue engineering. *Biomaterials*, 2006, **27**, 2414–2425.
17. Du, C., Cui, F. Z., Zhang, W., Feng, Q. L., Zhu, X. D. and De Groot, K., Formation of calcium phosphate/collagen composites

through mineralization of collagen matrix. *J. Biomed. Mater. Res. A*, 2000, **50**, 518–527.
18. Kikuchi, M., Itoh, S., Ichinose, S., Shinomiya, K. and Tanaka, J., Self-organization mechanism in a bone-like hydroxyapatite/collagen nanocomposite synthesized *in vitro* and its biological reaction *in vivo*. *Biomaterials*, 2001, **22**, 1705–1711.
19. Ahmad, Z. and Mark, J. E., Biomimetic materials: Recent developments in organic–inorganic hybrids. *Mater. Sci. Eng. C*, 1998, **6**, 183–196.
20. Xuan, C., Hua, T., Xinyu, S., Weixuan, Chen., Juan, Y. and Jiming, H., Preparation and characterization of homogeneous chitosan–polylactic acid/hydroxyapatite nanocomposite for bone tissue engineering and evaluation of its mechanical properties. *Acta Biomaterialia*, 2009, **5**, 2693–2703.
21. Hench, L. L. and Polak, J. M., Third-generation biomedical materials. *Science*, 2002, **295**, 1014–1017.
22. Xynos, I. D., Edgar, A. J., Buttery, L. D. K., Hench, L. L. and Polak, M., Gene expression profiling of human osteoblasts following treatment with the ionic products of Bioglass® 45S5 dissolution. *J. Biomed. Mater. Res*., 2001, **55**, 151–157.
23. Marcacci, M., Kon, E., Moukhachev, V., Lavroukov, A., Kutepov, S. and Quarto, R., Stem cells associated with macroporous bioceramics for long bone repair: 6- to 7-year outcome of a pilot clinical study. *Tissue Eng*., 2007, **13**, 947–955.
24. Mi, F. L., Tan, Y. C., Liang, H. F. and Sung, H. W., *In vivo* biocompatibility and degradability of a novel injectable-chitosan-based implant. *Biomaterials*, 2002, **23**, 181–191.
25. Wang, L. and Li, C. Z., Preparation and physicochemical properties of a novel hydroxyapatite/chitosan–silk fibroin composite. *Carbohydr. Polym*., 2007, **68**, 740–745.
26. Madihally, S. V. and Matthew, H. W. T., Porous chitosan scaffolds for tissue engineering. *Biomaterials*, 1999, **20**, 1133–1142.
27. Hutmacher, D. W., Scaffolds in tissue engineering bone and cartilage. *Biomaterials*, 2000, **21**, 2529–2543.
28. Wang, L. S., Khor, E., Wee, A. and Lim, L. Y., Chitosan–alginate PEC membrane as a wound dressing: assessment of incisional wound healing. *J. Biomed. Mater. Res. B*, 2002, **63**, 610–618.
29. Li, Z. S., Ramay, H. R., Hauch, K. D., Xiao, D. M. and Zhang, M. Q., Chitosan–alginate hybrid scaffolds for bone tissue engineering. *Biomaterials*, 2005, **26**, 3919–3928.
30. Jayachandran, V. and Se-Kwon, K., Chitosan composites for bone tissue engineering – an overview. *Mar. Drug*., 2010, **8**, 2252–2266.
31. Verma, D., Katti, K. S., Katti, D. R. and Mohanty, B., Mechanical response and multilevel structure of biomimetic hydroxyapatite/polygalacturonic/chitosan nanocomposites. *Mater. Sci. Eng. C*, 2008, **28**, 399–405.
32. Jiang, L. Y., Li, Y. B., Zhang, L. and Liao, J. G., Preparation and properties of a novel bone repair composite: nano-hydroxyapatite/chitosan/carboxymethyl cellulose. *J. Mater. Sci. Mater. Med*., 2008, **19**, 981–987.
33. Ashok, K. and Akshay, S., Cell separation using cryogel-based affinity chromatography. *Nature Protocols*, 2010, **5**, 1737–1747.
34. Zhang, L., Li, Y. B., Yang, A. P., Peng, X. L., Wang, X. J. and Zhang, X., Preparation and *in vitro* investigation of chitosan/nano-hydroxyapatite composite used as bone substitute materials. *J. Mater. Sci. Mater. Med*., 2005, **16**, 213–219.
35. Ali, N. N., Rowe, J. and Teich, N. M., Constitutive expression of nonbone/liver/kidney alkaline phosphatase in human osteosarcoma cell lines. *J. Bone Miner Res*., 1996, **11**, 512–520.
36. Yamaguchi, I., Tokuchi, K., Fukuzaki, H., Koyama, Y., Takakuda, K., Monma, H. and Tanaka, J., Preparation and microstructure analysis of chitosan/hydroxyapatite nanocomposites. *J. Biol. Mater. Res*., 2001, **55**, 20–27.
37. Wang, L., Nemoto, R. and Senna, M., Microstructure and chemical states of hydroxyapatite/silk fibroin nanocomposites synthesized via a wet-mechanochemical route. *J. Nanopart. Res*., 2002, **4**, 535–540.
38. Zhang, L., Li, Y. B., Yang, A. P., Peng, X. L., Wang, X. J. and Zhang, X., Preparation and *in vitro* investigation of chitosan/nano-hydroxyapatite composite used as bone substitute materials. *J. Mater. Sci. Mater. Med*., 2005, **16**, 213–219.

ACKNOWLEDGMENT. This work was fully supported by the 2009 Yeungnam University research grant.

Received 20 February 2012; revised and accepted 2 July 2012

Smile with Science

By – Santosh Kumar Sharma
santosh_ujj@yahoo.com